AD-A161 696 BEAM TRAPPING IN A MODIFIED BETATRON WITH TORSATRON WINDINGS(U) NAVAL RESEARCH LAB WASHINGTON DC C A KAPETANAKOS ET AL. 05 NOV 85 NRL-MR-5619 1/1

UNCLASSIFIED F/G 20/7 NL

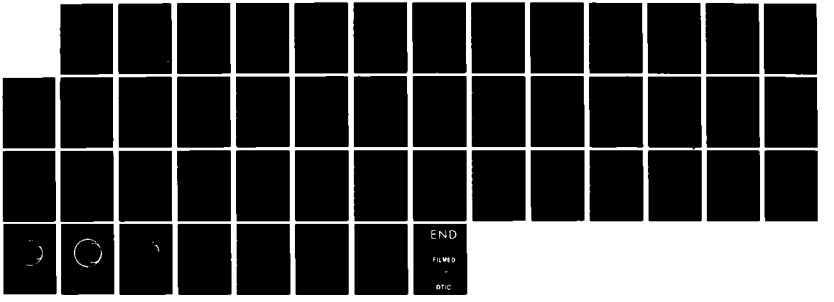

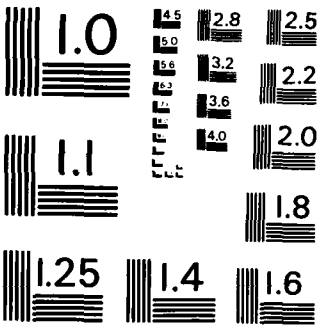

NRL Memorandum Report 5619

Beam Trapping in a Modified Betatron with Torsatron Windings

C. A. KAPETANAKOS

Advanced Beam Technologies Branch
Plasma Physics Division

D. DIALETIS

Science Appplications International Corporation
McLean, VA 22102

S. J. MARSH

Sachs/Freeman Associates
Bowie, MD 20715

November 5, 1985

NAVAL RESEARCH LABORATORY
Washington, D.C.

AD-A161 696

SECURITY CLASSIFICATION OF THIS PAGE

REPORT DOCUMENTATION PAGE

1a REPORT SECURITY CLASSIFICATION UNCLASSIFIED	1b RESTRICTIVE MARKINGS
2a SECURITY CLASSIFICATION AUTHORITY	3 DISTRIBUTION/AVAILABILITY OF REPORT Approved for public release; distribution unlimited.
2b DECLASSIFICATION/DOWNGRADING SCHEDULE	
4 PERFORMING ORGANIZATION REPORT NUMBER(S) NRL Memorandum Report 5619	5 MONITORING ORGANIZATION REPORT NUMBER(S)
6a NAME OF PERFORMING ORGANIZATION Naval Research Laboratory 6b OFFICE SYMBOL (If applicable) Code 4710	7a NAME OF MONITORING ORGANIZATION Office of Naval Research
6c ADDRESS (City, State, and ZIP Code) Washington, DC 20375-5000	7b ADDRESS (City, State, and ZIP Code) Arlington, VA 22217
8a NAME OF FUNDING/SPONSORING ORGANIZATION ONR and SDIO 8b OFFICE SYMBOL (If applicable)	9 PROCUREMENT INSTRUMENT IDENTIFICATION NUMBER
8c ADDRESS (City, State, and ZIP Code) Arlington, VA 22217 Washington, DC 20301-7100	10 SOURCE OF FUNDING NUMBERS PROGRAM ELEMENT NO: 61153N; PROJECT NO:; TASK NO: RR011-09-4B; WORK UNIT ACCESSION NO: DN280-013

11 TITLE (Include Security Classification)

Beam Trapping in a Modified Betatron with Torsatron Windings

12 PERSONAL AUTHOR(S)
Kapetanakos, C.A., Dialetis, D.* and Marsh, S.J.†

13a TYPE OF REPORT	13b TIME COVERED	14 DATE OF REPORT (Year, Month, Day)	15 PAGE COUNT
Interim	FROM _____ TO _____	1985 November 5	48

16 SUPPLEMENTARY NOTATION *Science Applications International Corporation, McLean, VA 22102
†Sachs/Freeman Associates, Bowie, MD 20715

17 COSATI CODES		
FIELD	GROUP	SUB-GROUP

18 SUBJECT TERMS (Continue on reverse if necessary and identify by block number)
Accelerators, Strong focusing
Modified betatron, ✓

19 ABSTRACT (Continue on reverse if necessary and identify by block number)

The guiding center equations for the reference electron that is located at the centroid of an intense electron ring confined in a torsatron assisted modified betatron field are derived by time averaging out its fast motion. These "slow" equations are integrated analytically to obtain the nonlinear orbits for the guiding center. In addition, from the guiding center equations we have obtained a nonlinear expression that predicts very accurately the ring equilibrium position even for large displacement from the minor axis of the torus. These results have provided an invaluable insight in the development of a trapping scheme. The proposed scheme is compatible with the slow acceleration of the modified betatron and is based on a low amplitude, rapidly varying magnetic field that shifts the ring equilibrium position from near the wall to the minor axis of the torus in time shorter than a beam bounce period.

20 DISTRIBUTION/AVAILABILITY OF ABSTRACT	21 ABSTRACT SECURITY CLASSIFICATION
☒ UNCLASSIFIED/UNLIMITED ☐ SAME AS RPT ☐ DTIC USERS	UNCLASSIFIED
22a NAME OF RESPONSIBLE INDIVIDUAL C. A. Kapetanakos	22b TELEPHONE (Include Area Code) (202) 767-2838 22c OFFICE SYMBOL Code 4710

DD FORM 1473, 84 MAR 83 APR edition may be used until exhausted
All other editions are obsolete

SECURITY CLASSIFICATION OF THIS PAGE

CONTENTS

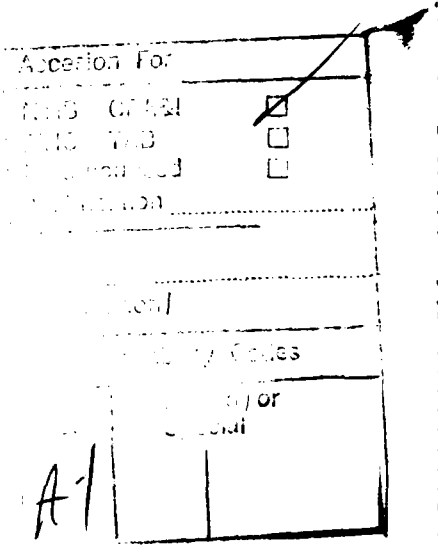

BEAM TRAPPING IN A MODIFIED BETATRON WITH TORSATRON WINDINGS

I. Introduction

Extensive theoretical studies[1-20] over the last few years have shown that the modified betatron accelerator has the potential to generate very high current electron beams. Recently, a "table top" device[21] at the University of California, Irvine has produced electron rings with about 200A circulating current. A larger device, currently under testing at the Naval Research Laboratory,[22] has been designed to produce multi-kiloampere electron rings and to address the critical physics issues of the modified betatron concept.

A disadvantage of the modified betatron accelerator is its sensitivity to the energy mismatch.[2] Whenever the energy of the electron beam is not precisely matched to the betatron magnetic field, the center of gyration or equilibrium position of the beam in the transverse to the minor axis plane is shifted radially and thus the probability for the beam to strike the wall is increased. To alleviate the energy mismatch problems, a modified betatron accelerator should be carefully designed to provide both an accurate and precise betatron field and the injector accelerator should generate electron pulses having energy that precisely matches this field.[22]

To reduce the orbit sensitivity of the modified betatron to the energy mismatch, Roberson[23] et al. have suggested the use of a strong focusing field generated by $\ell = 2$ stellarator windings. In more recent studies,[24] we have demonstrated numerically that the energy bandwidth of a modified betatron configuration assisted by a strong focusing field generated by torsatron windings can be very wide. In addition, we have shown that the torsatron windings also substantially improve the current carrying capabilities of the device[24] and could alleviate the beam displacement problem associated with the diffusion of the self magnetic field.

Manuscript approved July 2, 1985.

However, the usefulness of the twisted windings in improving the performance of the modified betatron remained questionable, because a scheme to trap the beam in such a configuration was not available. By reducing the orbit sensitivity to the energy mismatch, the strong focusing field made the beam trapping into such devices more difficult.

Recently Sprangle and Kapetanakos[25] have developed a scheme for trapping a beam into a rebatron accelerator. This device has a magnetic field configuration that is similar to that of a modified betatron supplemented with torsatron windings. The suggested scheme is based on the dissipative force generated by the resistive wall surrounding the electron ring. Although such a trapping scheme is appropriate for a rebatron, it is of doubtful usefulness for the modified betatron. The reason is that in the rebatron the particle acceleration occurs very rapidly, i.e., over a few μsec and therefore the cyclotron frequency corresponding to the betatron magnetic field ($\Omega_{z0/\gamma}$) very rapidly with time. Therefore, the resistive wall mode may not impose serious limitations on the stability of the ring. However, this is not the case in the modified betatron, because the acceleration occurs slowly, i.e., over a few msec.

In this paper we propose a trapping scheme that is compatible with the slow acceleration of the modified betatron. The proposed trapping approach is based on a low amplitude, rapidly varying magnetic field that shifts the beam equilibrium position near the minor axis of the torus in time shorter than the beam bounce period. Since the new trapping scheme is similar to that presently used in the NRL modified betatron,[13,14] its implementation would require only minor modifications in the existing device.

Before addressing the beam trapping, we will derive two equations that describe the nonlinear motion of the guiding center of the reference electron that is located at the beam

centroid. Using these equations we will obtain a nonlinear expression that predicts very accurately the beam equilibrium position, even for large displacement from the minor axis of the torus. In addition, by integrating analytically the guiding center equations we will obtain a constant of the motion that predicts accurately the topology of the guiding center orbits. These analytical results have provided an invaluable insight in the development and understanding of the trapping scheme.

II. Guiding Center Motion

In this Section we derive the equations describing the guiding center motion for the reference electron that is located at the centroid of a circular cross section electron beam. In the system of coordinates shown in Fig. 1, the instanteneous position of the reference electron is

$$r = r_0 + X + \delta r \quad , \tag{1}$$

$$z = Z + \delta z \quad , \tag{2}$$

where r_0 is the major radius of the torus, X and Z is the position of the guiding center relative to the minor axis and δr and δz give the position of the gyrating electron relative to the guiding center.

Introducing the complex variables

$$u = r + i z \quad , \tag{3}$$

$$U = X + i Z \quad , \tag{4}$$

$$\delta u = \delta r + i \delta z \quad , \tag{5}$$

and combining Eqs. (1) to (5), we obtain

$$u = r_o = U + \delta u \quad . \tag{6}$$

Substituting Eq. (3) and its time derivative into the equations of motion

$$\frac{d}{dt} (\gamma \dot{r}) - \gamma r \dot{\vartheta}^2 = - \frac{e}{m} \left(E_r + \frac{1}{c} (r \dot{\theta} B_z - \dot{z} B_\vartheta)\right) ,$$

and

$$\frac{d}{dt} (\gamma \dot{z}) = - \frac{e}{m} \left(E_z + \frac{1}{c} (\dot{r} B_\theta - r \dot{\vartheta} B_r)\right) ,$$

we obtain

$$\ddot{U} + (\frac{\dot{\gamma}}{\gamma} + i \frac{\Omega_\vartheta}{\gamma}) \dot{u} - \frac{v_\vartheta^2}{r} = - \frac{e}{m\gamma} \left((E_r + i E_z) - \frac{i v_\vartheta}{c} (B_r + i B_z)\right) , \tag{7}$$

where Ω_ϑ is the cyclotron frequency corresponding to the toroidal magnetic field, v_ϑ is the toroidal velocity, which is assumed constant, E_r and E_z are the image electric fields and B_r and B_z are the components of applied and image magnetic fields. The last terms consists of the torsatron, betatron and image magnetic fields.

(a) Applied Magnetic Fields

The toroidal magnetic field consists of the applied toroidal field and that generated by the torsatron windings. To lowest order the toroidal field is given by[24]

$$B_\vartheta = - (B_o + B_s^{ex}) + B_s^{ex} \epsilon_t I_2(2 \alpha o) \left(e^{2i(\vartheta - \alpha s)} + e^{-2i(\vartheta - \alpha s)}\right), \tag{8}$$

where B_o and B_s^{ex} are defined in the local coordinate system $\hat{e}_x$, $\hat{e}_y$, $\hat{e}_s$, $B_o = 8\pi I/cL$, I is the current and L is the period of the torsatron windings,

$B_s^{ex}\varepsilon_t = 2\alpha B_o \rho_o K_2'(2\alpha\rho_o)$, ρ_o is the minor radius of the torsatron windings, K_2 and I_2 are the modified Bessel functions and $\alpha = 2\pi/L$.

Since v_ϑ is assumed constant

$$\omega_w \equiv 2\alpha v_\vartheta = -2\alpha s/t, \tag{9}$$

and Eq. (8) becomes

$$B_\vartheta = -(B_o + B_s^{ex}) + B_s^{ex}\varepsilon_t I_2(2\alpha o)\left(e^{2i\phi}e^{i\omega_w t} + e^{-2i\phi}e^{-i\omega_w t}\right). \tag{10}$$

Similarly, to the lowest order the components of the torsatron field transverse to the minor axis are[24]

$$B_o^t = 2B_s^{ex}\varepsilon_t I_2'(2\alpha\rho)\sin\left[2(\phi - \alpha s)\right], \tag{11}$$

$$B_\phi^t = \frac{2B_s^{ex}\varepsilon_t}{\alpha o} I_2(2\alpha o)\cos\left[2(\phi - \alpha s)\right]. \tag{12}$$

Substituting Eqs. (11) and (12) into Eqs. (13) and (14)

$$B_r^t = B_o^t\cos\phi - B_\phi^t\sin\phi \tag{13}$$

$$B_z^t = B_\rho^t\sin\phi + B_\phi^t\cos\phi, \tag{14}$$

and using Eq. (9), we obtain

$$(B_r^t + i B_z^t) = B_s^{ex} \varepsilon_t \, i \left(I_1 (2 \alpha \rho) e^{-i\phi} e^{-i\omega_w t} - I_3 (2 \alpha \rho) e^{3i\phi} e^{i\omega_w t} \right). \qquad (15)$$

In addition to the torsatron field, the betatron field contributes to the last term of Eq. (7). Assuming that the betatron field components vary as

$$B_r^b \approx - B_{zo} \frac{nz}{r_o} ,$$

$$B_z^b \approx B_{zo} \left(1 - \frac{n (r-r_o)}{r_o} \right) ,$$

we obtain

$$(B_r^b + i B_z^b) = i B_{zo} \left(1 + n - \frac{n}{r_o} (r - i z) \right), \qquad (16)$$

where B_{zo} is the betatron field on the minor axis and n is the external field index.

(b) Image Fields at the Ring Centroid

An accurate self consistent determination of self fields of a high current electron ring in a modified betatron configuration that is supplemented by strong focusing is very difficult, because the minor cross section of the ring varies along the toroidal direction.

However, here we are interested in the macroscopic motion of the ring and therefore on the image fields that act on the ring centroid. These fields are not sensitive to the detailed shape

of the ring cross section and thus can be computed approximately assuming that the ring has a circular cross section that is uniformly filled. Neglecting toroidal corrections, the fields at the reference particle are

$$B_\phi = \frac{2\, e n_o v_\vartheta \pi\, r_b^2\, \rho_o}{a^2 c\, (1 - \rho^2/a^2)}\,, \tag{17}$$

$$E_\rho = -\frac{2\, e n_o\, \pi\, r_b^2\, \rho}{a^2\, (1 - \rho^2/a^2)}\,, \tag{18}$$

where r_b is the minor radius of the ring, a is the minor radius of the perfectly conducting torus and n_o is the uniform electron density.

Since

$$B_r = -B_\phi \sin\phi \qquad \text{and} \qquad E_r = E_\rho \cos\phi$$
$$B_r = B_\phi \cos\phi \qquad\qquad E_z = E_\rho \sin\phi\,,$$

Eqs. (17) and (18) give

$$-\frac{e}{m}\left[(E_r + i E_z) - i\beta_\vartheta (B_r + i B_z)\right] = \frac{\omega_p^2}{2}\left(\frac{r_b}{a}\right)^2 \frac{(X+\delta r) + i(Z+\delta z)}{(1 - \rho^2/a^2)\gamma^2}\,. \tag{19}$$

(c) Taylor Series Expansion of the Fields

To separate the slow from the fast motion of the reference electron it is necessary to Taylor expand the fields about the guiding center. Neglecting terms higher than quadratic, we have

$$B(r,z) \cong B(R,\phi) + \overrightarrow{\delta\rho} \cdot \nabla B\big|_{R,\phi}$$

$$= B(R,\phi) + \frac{1}{2}(\delta u + \delta u^*)\frac{\partial B}{\partial X} + \frac{1}{2i}(\delta u - \delta u^*)\frac{\partial B}{\partial Z} . \qquad (20)$$

Since

$$X = R\cos\phi \text{ and } Z = R\sin\phi,$$

$$\frac{\partial}{\partial R} = \frac{\partial X}{\partial R}\frac{\partial}{\partial X} + \frac{\partial Z}{\partial R}\frac{\partial}{\partial Z} = \cos\phi\frac{\partial}{\partial X} + \sin\phi\frac{\partial}{\partial Z},$$

and

$$\frac{\partial}{\partial \phi} = \frac{\partial X}{\partial \phi}\frac{\partial}{\partial X} + \frac{\partial Z}{\partial \phi}\frac{\partial}{\partial Z} = -R\sin\phi\frac{\partial}{\partial X} + R\cos\phi\frac{\partial}{\partial Z},$$

Eq. (20) becomes

$$B(r,z) \cong B(R,\phi) + \frac{1}{2}\delta u\, e^{-i\phi}\left(\frac{\partial}{\partial R} - \frac{i}{R}\frac{\partial}{\partial \phi}\right)B + \frac{1}{2}\delta u^* e^{i\phi}\left(\frac{\partial}{\partial R} + \frac{i}{R}\frac{\partial}{\partial \phi}\right)B. \qquad (21)$$

Furthermore, we will assume that the reference electron rotates around the guiding center with frequency $\pm \omega_w$ i.e.,

$$\delta u = \delta u_+ e^{i\omega_w t} + \delta u_- e^{-i\omega_w t}. \tag{22}$$

This assumption is supported by the following two observations. We have shown[24] that when $\omega_w << \Omega_\theta/\gamma$, ω_w is an eigenfrequency of the linear system and that

$\omega_w >> \omega_s \equiv (\Omega_s^{ex} \varepsilon_t/\gamma)^2/4\ (1 - \Omega_\theta/\gamma\omega_w)\ (\Omega_\theta/\gamma)$, where ω_s is the slowest eigenmode of the linear system. In addition, extensive numerical results show that when $\omega_w << \Omega_\theta/\gamma$ the electrons gyrate around the guiding center at ω_w.

The time derivative of Eq. (22) is

$$\delta\dot{u} = i\omega_w (\delta u_+ e^{i\omega_w t} - \delta u_- e^{-i\omega_w t}) \tag{23}$$

$$+ \vec{R} \cdot \nabla (\delta u_+ e^{i\omega_w t} + \delta u_- e^{-i\omega_w t}).$$

We will show later that $\delta u_+ \sim I_3 (2 \alpha \rho)$ and $\delta u_- \sim I_1 (2 \alpha \rho)$ and therefore $\nabla \delta u_\pm \sim 2\alpha \delta u_\pm$. The second term in Eq. (23) can be neglected, provided

$$\dot{R} \cdot \nabla \delta u_\pm \ll \omega_w \delta u_\pm, \text{ or}$$
$$\dot{U} \ll v_\vartheta. \tag{24}$$

(d) Time Averaged Equations

Substituting into Eq. (7) the Taylor expanded fields of Eqs. (10), (15), (16) and (19) using expression (21), omitting terms quadratic in δu, multiplying the resulting equation by $e^{im\omega_w t}$, taking time average from o to $2\pi/\omega_w$, and omitting the small term $\langle \ddot{U} \; e^{im\omega_w t} \rangle$, we obtain for m=o.

$$\frac{\dot{\gamma}}{\gamma}\dot{U} - \frac{i\dot{U}}{\gamma}\left(\Omega_o + \frac{\Omega_{so}^{ex} r_o}{r_o + X}\right) + i\frac{v_\vartheta \alpha}{\gamma}\Omega_s^{ex}\varepsilon_t \left(\frac{\dot{U}}{v_\vartheta} f_1 - if_2\right)\delta u_- + \frac{iv_\vartheta}{\gamma}\alpha\Omega_s^{ex}\varepsilon_t\left(\frac{\dot{U}}{v_\vartheta} f_3^* + if_2^*\right)\delta u_+ + \frac{iv_\vartheta\alpha}{\gamma}\Omega_s^{ex}\varepsilon_t\left(\frac{\dot{U}}{v_\vartheta} f_1^* - if_o\right)\delta u_- + \frac{iv_\vartheta\alpha}{\gamma}\Omega_s^{ex}\varepsilon_t\left(\frac{\dot{U}}{v_\vartheta} f_3 + if_4\right)\delta u_+^* = \frac{\omega_p^2}{2}\left(\frac{r_b}{a}\right)^2 \frac{(X + iZ)}{(1 - R^2/a^2)\gamma^3} + \frac{v_a^2}{r_o + X} - \left(\frac{v_\vartheta}{\gamma}\right)\Omega_{zo}\left(1 - \frac{n}{r_o}(X - iZ)\right), \tag{25}$$

where

$$f_n (R, \Phi) \equiv I_n (2 \alpha R) e^{in\Phi}.$$

In addition, for m=1 the time averaged equation is

$$- \omega_w \Big(\omega_w + \frac{\dot{\gamma}}{\gamma} i + \frac{1}{\gamma} \Big(\Omega_o + \frac{\Omega_{so}^{ex} r_o}{r_o + X} \Big) - \frac{i \dot{U}}{2 \gamma \omega_w} \frac{\Omega_{so}^{ex} r_o}{(r_o + X)^2} -$$

$$\frac{v_\theta^2}{2 (r_o + X)^2 \omega_w} + \frac{1}{2} \frac{\omega_p^2}{\gamma^3 \omega_w} \Big(\frac{r_b}{a} \Big)^2 \frac{1}{(1 - R^2/\alpha^2)^2} \Big) \delta u_-$$

$$- \Big(\frac{v_\theta}{\gamma} \frac{n}{r_o} \Omega_{zo} + \frac{1}{2} \frac{\omega_p^2}{\gamma^3} \Big(\frac{r_b}{\alpha} \Big)^2 \frac{\Big(\frac{X}{\alpha} + i \frac{Z}{\alpha} \Big)^2}{(1 - R^2/\alpha^2)^2}$$

$$- \frac{i \dot{U}}{2 \gamma} \frac{\Omega_{so}^{ex} r_o}{(r_o + X)^2} - \frac{v_\theta^2}{2 (r_o + X)^2} \Big) \delta u_+^*$$

$$= - \frac{\Omega_s^{ex} \varepsilon_t}{\gamma} \left(v_\theta f_1^* + i \dot{U} f_2^* \right) . \qquad (26)$$

Similarly, for m = - 1, the time averaged equation gives

$$-\left(\frac{v_\theta}{\gamma} \frac{n}{r_o} \Omega_{zo} + \frac{1}{2} \underline{\frac{\omega_p^2}{\gamma^3} \left(\frac{r_b}{\alpha}\right)^2 \frac{\left(\frac{X}{\alpha} + i \frac{Z}{\alpha}\right)^2}{\left(1 - R^2/\alpha^2\right)^2}} - \underline{\frac{v_\theta^2}{2(r_o + X)^2}} - \right.$$

$$\left. \underline{\frac{i \dot{U}}{2 \gamma} \frac{\Omega_{so}^{ex} r_o}{(r_o + X)^2}} \right) \delta u_-^*$$

$$- \omega_w \left(\omega_w - \frac{\dot{\gamma}}{\gamma} i - \underline{\frac{i \dot{U}}{2 \gamma \omega_w} \frac{\Omega_{so}^{ex} r_o}{(r_o + X)^2}} - \underline{\frac{v_\theta^2}{2 (r_o + X)^2 \omega_w}} + \right.$$

$$\frac{\omega_p^2}{2 \omega_w \gamma^3} \left(\frac{r_b}{a}\right)^2 \frac{1}{(1 - R^2/a^2)^2}$$

$$\left. - \frac{1}{\gamma} \left(\Omega_o + \frac{\Omega_{so}^{ex} r_o}{r_o + X} \right) \right) \delta u_+ = \frac{v_\theta}{\gamma} \Omega_s^{ex} \varepsilon_t f_3 - \underline{\frac{i \dot{U}}{\gamma} \Omega_s^{ex} \varepsilon_t f_2} . \quad (27)$$

For the parameters of interest, the underlined terms in Eqs. (26) and (27) are small in comparison with the non-underlined terms and therefore can be omitted.

In addition, assuming that $\dot{\gamma}/\gamma << \omega_w$, , Eqs. (26) and (27) give

$$\delta u_- = \frac{(v_{\theta/\gamma})^2 \frac{n}{r_o} \Omega_{zo} \Omega_s^{ex} \varepsilon_t f_3^* + f_1 (v_{\theta/\gamma}) \Omega_s^{ex} \varepsilon_t \omega_w \left(\Omega_w + \hat{\Omega}_{\theta/\gamma} \right)}{\omega_w^2 \left(\Omega_w^2 - \hat{\Omega}_\theta^2 / \gamma^2 \right)} \simeq$$

$$\frac{f_1^* \ (v_{\theta/\gamma}) \ \Omega_s^{ex} e_t}{\omega_w \ (\Omega_w - \hat{\Omega}_{\theta/\gamma})} \ , \tag{28}$$

and

$$\delta u_+^* = \frac{-(v_{\theta}/\gamma) \ \Omega_s^{ex} \ \varepsilon_t (f_3^* \ \omega_w \ (\Omega_w - \hat{\Omega}_{\theta/\gamma}) + f_1^* \ (v_{\theta/\gamma}) \ \Omega_{zo} \ n/r_o)}{\omega_w^2 \ (\Omega_w^2 - \hat{\Omega}_{\theta}^2/\gamma^2) - \left(\frac{v_{\theta} n}{r_o} \frac{\Omega_{zo}}{\gamma}\right)^2} \approx$$

$$- \frac{(v_{\theta/\gamma}) \ \Omega_s^{ex} \ \varepsilon_t \ f_3^*}{\omega_w \ (\Omega_w + \hat{\Omega}_{\theta/\gamma})} \ , \tag{29}$$

where

$$\Omega_w \equiv \omega_w + \frac{1}{2} \frac{\omega_p^2}{\gamma^3 \omega_w} \left(\frac{r_b}{a}\right)^2 \frac{1}{(1 - R^2/a^2)^2} \quad \text{and}$$

$$\hat{\Omega}_{\theta} = - \left(\Omega_o + \frac{\Omega_{so}^{ex} r_o}{r_o + X} \right) .$$

Substituting $\delta u_{\pm}$ from (28) and (29) into the equation for the slow motion [Eq. (25)], we obtain

$$\dot{Z} + \frac{v_{\theta} \ (\Omega_s^{ex} \varepsilon_t/\gamma)^2 \ [I_2 \ (2\alpha R) + I_o \ (2\alpha R) \ ] I_1 \ (2\alpha R) \ X}{2 \ (\hat{\Omega}_{\theta}/\gamma) \ (\hat{\Omega}_{\theta}/\gamma - \Omega_w)} \ \frac{}{R} \ -$$

$$\frac{v_\theta \left(\Omega_s^{ex} \epsilon_{t/\gamma}\right)^2 \left[I_2(2\alpha R) + I_4(2\alpha R)\right] I_3(2\alpha R)\, X}{2\left(\hat{\Omega}_{\theta/\gamma}\right)\left(\hat{\Omega}_{\theta/\gamma} + \Omega_w\right) R}$$

$$= - \frac{v_\theta^2}{\left(\hat{\Omega}_{\theta/\gamma}\right)(r_o + X)} + \frac{v_\theta \left(\Omega_{zo/\gamma}\right)}{\left(\hat{\Omega}_{\theta/\gamma}\right)} \left(1 - \frac{n}{r_o} X\right)$$

$$- \frac{\omega_p^2}{2\left(\hat{\Omega}_{\theta/\gamma}\right)} \left(\frac{r_b}{a}\right)^2 \frac{X}{\left(1 - R^2/a^2\right) \gamma^3}, \qquad (30)$$

and

$$\dot{X} - \frac{v_\theta \left(\Omega_s^{ex} \epsilon_{t/\gamma}\right)^2 \left[I_2(2\alpha R) + I_0(2\alpha R)\right] I_1(2\alpha R)\, Z}{2\left(\hat{\Omega}_{\theta/\gamma}\right)\left(\hat{\Omega}_{\theta/\gamma} - \Omega_w\right) R} +$$

$$\frac{v_\theta \left(\Omega_s^{ex} \epsilon_{t/\gamma}\right)^2 \left[I_2(2\alpha R) + I_4(2\alpha R)\right] I_3(2\alpha R)\, Z}{2\left(\hat{\Omega}_{\theta/\gamma}\right)\left(\hat{\Omega}_{\theta/\gamma} + \Omega_w\right) R}$$

$$= - \frac{n\, v_\theta \left(\Omega_{zo/\gamma}\right)}{\left(\hat{\Omega}_{\theta/\gamma}\right)} \frac{Z}{r_o} + \frac{\omega_p^2}{2\left(\hat{\Omega}_{\theta/\gamma}\right)} \left(\frac{r_b}{a}\right)^2 \frac{Z}{\left(1 - R^2/a^2\right)\gamma^3}. \qquad (31)$$

These are the nonlinear equations that describe the guiding center motion for the reference electron. The guiding center gyrates around the equilibrium position X_o, which can be determined from (30) and (31) by taking $\dot{X} = \dot{Z} = o$ and is given by the expression

$$- \frac{(\Omega_s^{ex}\varepsilon_t/\gamma)^2 [I_0(2\alpha X_0) + I_2(2\alpha X_0)] I_1(2\alpha X_0)}{2(\Omega_{zo}/\gamma)\left(\frac{\Omega_0}{\gamma} + \frac{\Omega_{so}^{ex} r_0}{\gamma(r_0 + X_0)} + \Omega_w\right)} +$$

$$\frac{(\Omega_s^{ex}\varepsilon_{t/\gamma})^2}{2(\Omega_{zo/\gamma})} \frac{[I_2(2\alpha X_0) + I_4(2\alpha X_0)] I_3(2\alpha X_0)}{\left[\Omega_0/\gamma + \frac{\Omega_{so}^{ex} r_0}{\gamma(r_0 + X)} - \Omega_w\right]}$$

$$= - \frac{v_\vartheta}{(r_0 + X_0)(\Omega_{zo/\gamma})} + (1 - \frac{n}{r_0} X_0)$$

$$= \frac{\omega_p^2}{2(\Omega_{zo/\gamma})} \left(\frac{r_b}{a}\right)^2 \frac{1}{v_\vartheta} \frac{X_0}{(1 - X_0^2/a^2)\gamma^3} \qquad (32)$$

(e) Integration of Nonlinear Equations

The nonlinear equations (30) and (31) can be integrated, provided that the spatial variation of $\hat{\Omega}_\theta$ and Ω_w can be neglected, i.e., when $\hat{\Omega}_\theta = \hat{\Omega}_{\theta o}$ = constant and $\Omega_w = \Omega_{wo}$ = constant.

Multiplying Eq. (30) by $\dot{X}$ and (31) by $\dot{Z}$ and taking their difference, we obtain

$$0 = - \frac{v_\vartheta(\Omega_s^{ex}\varepsilon_{t/\gamma})^2 [I_0(2\alpha R) + I_2(2\alpha R)] I_1(2\alpha R)}{2(\hat{\Omega}_{\theta o/\gamma})(\hat{\Omega}_{\theta o/\gamma} - \Omega_{wo})} \frac{1}{R} \frac{1}{2} \frac{d}{dt}(R^2)$$

$$+ \frac{v_\vartheta(\Omega_s^{ex}\varepsilon_{t/\gamma})^2 [I_2(2\alpha R) + I_4(2\alpha R)] I_3(2\alpha R)}{2(\hat{\Omega}_{\theta o/\gamma})(\hat{\Omega}_{\theta o/\gamma} + \Omega_{wo})} \frac{1}{R} \frac{1}{2} \frac{d}{dt}(R^2)$$

$$- \frac{\omega_p^2}{2\,(\hat{\Omega}_{\theta 0/\gamma})} \left(\frac{r_b}{a}\right)^2 \quad \frac{\frac{1}{2}\,\frac{d}{dt}(X^2 + Z^2)}{(1 - R^2/a^2)\,\gamma^3}$$

$$- \frac{v_\theta^2}{(\hat{\Omega}_{\theta 0/\gamma})} \frac{d}{dt} \ln\,(1 + X/r_0) + \frac{v_\theta(\Omega_{z0}/\gamma)}{(\hat{\Omega}_{\theta 0/\gamma})} \frac{d}{dt}\left(X - \frac{\eta}{2r_0}X^2\right)$$

$$+ \frac{(v_\theta/\gamma)\,\Omega_{z0}}{2\,(\hat{\Omega}_{\theta 0/\gamma})} \quad \frac{\eta}{r_0} \quad \frac{d}{dt}\,(Z^2)\,. \tag{33}$$

The integration of the last four terms in Eq. (33) is elementary. To integrate the first term, we write

$$\left(I_0\,(2\alpha R) + I_2\,(2\alpha R)\right)\, I_1\,(2\alpha R) \equiv \frac{d\psi_1}{dr}\,,$$

where ψ_1 is a function to be determined.

Since

$$\frac{d\psi_1}{dt} = \frac{d\psi_1}{dr} \quad \frac{dR}{dt} = (I_0 + I_2)\, I_1 \frac{dR}{dt}\,, \tag{34}$$

the function ψ_1 is obtained from

$$\psi_1 = \int I_0 (2\alpha R)\, I_1 (2\alpha R)\, dR + \int I_2(2\alpha R)\, I_1(2\alpha R)\, dR = \frac{I_1^2}{2\alpha} \quad . \qquad (35a)$$

Similarly, the second term gives

$$\psi_2 = \int I_2 (2\alpha R)\, I_3(2\alpha R)\, dR + \int I_4(2\alpha R) I_3(2\alpha R)\, dR = I_3^2/_{2\alpha} \qquad (35b)$$

Substituting Eqs. (34) and (35) into Eq. (33) and carrying out the time integration, we obtain

$$\hat{K} = - \frac{v_\theta\, (\Omega_s^{ex}\, \varepsilon_{t/\gamma})^2}{2\, (\hat{\Omega}_{\theta o}/\gamma)(\hat{\Omega}_{\theta o}/\gamma - \Omega_{wo})} \frac{I_1^2 (2\alpha R)}{2\alpha} + \frac{v_\theta (\Omega_s^{ex} \varepsilon_{t/\gamma})^2}{2(\hat{\Omega}_{\theta o}/\gamma)\, (\hat{\Omega}_{\theta o}/\gamma + \Omega_{wo})} \frac{I_3^2(2\alpha R)}{2\alpha}$$

$$+ \frac{\omega_p^2\, a^2}{4\, \left(\frac{\hat{\Omega}_{\theta o}}{\gamma}\right) \gamma^3} \left(\frac{r_b}{a}\right)^2 \ln\, (1 - R^2/_{a^2})$$

$$- \frac{v_\theta^2}{(\hat{\Omega}_{\theta o/\gamma})} \ln\, (1 + \frac{X}{r_o}) + \frac{v_\theta (\Omega_{zo/\gamma})}{(\hat{\Omega}_{\theta o/\gamma})} \left(X - \frac{n}{2r_o} (X^2 - Z^2) \right), \qquad (36)$$

where $\hat{K}$ is a constant, $\hat{\Omega}_{\theta o} = -\, (\Omega_o + \Omega_{so}^{ex})$ = constant and

$$\Omega_{wo} = \omega_w + \frac{1}{2} \frac{\omega_p^2}{\gamma^3 \omega_w} \left(\frac{r_b}{a}\right)^2 = \text{constant}$$

Defining a new constant $K = -\hat{K}\left(\frac{2\hat{\Omega}_{\theta o}}{v_\theta \Omega_{zo} r_o}\right)$, Eq. (36) becomes

$$K = \frac{(\Omega_s^{ex} \varepsilon_{t/\gamma})^2 I_1^2 (2\alpha R)}{2\alpha r_o (\Omega_{zo/\gamma})(\hat{\Omega}_{\theta o/\gamma} - \Omega_{wo})} - \frac{(\Omega_s^{ex} \varepsilon_t/\gamma)^2 I_3^2 (2\alpha R)}{2 r_o \alpha (\Omega_{zo}/\gamma)(\hat{\Omega}_{\theta o}/\gamma + \Omega_{wo})}$$

$$- \frac{\omega_p^2}{2\gamma^3 (v_\theta/r_o)(\Omega_{zo}/\gamma)} (r_b/r_o)^2 \ell n (1 - R^2/a^2)$$

$$+ \frac{2 (v_\theta/r_o)}{(\Omega_{zo}/\gamma)} \ell n (1 + X/r_o) - [2 X/r_o - n (X^2 - Z^2)/r_o^2]. \quad (38)$$

Equation (38) describes the nonlinear, slow motion of the beam centroid in the transverse to the minor axis plane. the constant K is determined from the initial conditions and in order the orbit to pass through the minor axis (X = Z = o) K should be zero.

Near the minor axis, i.e., when $2\alpha R << 1$ and $R/a << 1$,

Eq. (38) can be linearized and the resulting expression, when the small term that contains I_3 is omitted, is

$$K = \frac{(\Omega_s^{ex} \varepsilon_{t/\gamma})^2 r_o \alpha}{2 (\Omega_{zo/\gamma})(\hat{\Omega}_{\theta o/\gamma} - \hat{\Omega}_{wo})} (R/r_o)^2 + \frac{\omega_p^2 (r_{b/a})^2 (R/r_o)^2}{2(v_\theta/r_o)(\Omega_{zo/\gamma})\gamma^3}$$

$$+ 2 \left(X/r_o \right) \frac{\delta \gamma}{\gamma_o} + (X/r_o)^2 (n - 1) - \left(Z/r_o \right)^2 n \, . \qquad (39)$$

The displacement of the orbit center from the minor axis can be easily determined from (39) and is given by

$$\Delta r_{o/r_o} = \left(\delta\gamma/\gamma \right) \left\{ 1 - n - \frac{(\Omega_s^{ex} \varepsilon_{t/\gamma})^2 r_o \alpha}{2 (\Omega_{zo/\gamma}) (\hat{\Omega}_{\vartheta o/\gamma} - \hat{\Omega}_{wo})} - \right.$$

$$\left. \frac{\omega_p^2 (r_{b/a})^2}{2 (v_{\vartheta}/r_o) (\Omega_{zo/\gamma}) \gamma^3} \right\}^{-1}, \qquad (40)$$

where $\gamma_o = \frac{\Omega_{zo} r_o}{v_{\vartheta o}}$. and $\delta\gamma = \gamma - \gamma_o$ is the energy mismatch.

Equation (38) is plotted in Fig. 2a for various values of constant K, for zero electron beam density. The various parameters for the results of Fig. 2 are listed in Table I.

The number marked in every fourth macroscopic beam orbit is equal to 10^3 K. Orbits shown with solid lines correspond to K that is greater than zero and those shown with a dashed line correspond to K that is less than zero.

All the orbits close inside the vacuum chamber. However, those of them that lie less than a minor ring radius from the wall are not useful, because when the beam is moving along one of these orbits it will scrape the wall.

Figure 2 b shows an electron orbit obtained from the numerical integration of orbit equations superimposed on a macroscopic orbit of Fig. 2a that corresponds to the same conditions. In both, the numerically obtained orbit and the macroscopic orbit from the constant of the motion the toroidal corrections in the torsatron field have been omitted. It is quite obvious that the constant of the motion predicts accurately the guiding center motion. The period of the particle gyrating around the guiding center is about 1 nsec, in agreement with Eq. (22) and the radius of gyration decreases as the electron moves toward the minor axis, in agreement with Eqs. (28) and (29).

The predictions of the constant of the motion remain rather accurate even when the toroidal corrections of the torsatron field are included in the orbit equations. Results are shown in Fig. 3c.

For the values of the parameters listed in Table I, Eq. (32) predicts that the nonlinear equilibrium position is located at $X_0 \sim 10.2$ cm. To determine accurately the equilibrium position, we have repeated the computer run of Fig. 2a using a finer scale. The results are shown in Fig. 2d and indicate an equilibrium position that is very close to 10.2cm. To check these predictions, we made a computer run with the electron initially placed at X = 10.0 cm, Z = o. We have observed that the electron started to gyrate around the X = 10.25 cm, Z = o point with a radius of a few millimeters. This test demonstrates unequivocally that Eq. (32) predicts accurately the equilibrium position even when the parameter $2 \alpha R > 1$.

However, this is not the case with the linearized expression given by Eq. (40). For the parameters of Table I Eq. (40) predicts a $\Delta r_0 \tilde{=} 37$ cm, i.e., it overestimates the equilibrium position by about a factor of four.

(f) Toroidal Corrections

So far, we made the assumption that the aspect ratio a/r_o is very small and thus all the toroidal corrections associated with the fields have been neglected.

For devices with parmeters similar to those listed in Table I and II the toroidal corrections associated with the torsatron fields change only slightly the ring orbits as it is manifested by the results of Fig. 2c. Even with the torsatron field corrections, we were able to derive the two slow equations of motion, but we were unable to analytically integrate them and thus to derive a constant of the motion.

In contrast to the torsatron field, the toroidal corrections of the self fields become very important when the ring current reaches a few kiloamperes. In addition to changing the speed of rotation around the equilibrium position, the self field toroidal corrections modify the value of the vertical field required to confine the beam at its equilibrium position.

To lowest order, the self field toroidal corrections can be included in the slow equations of motion by replacing the last term in Eq. (30) by

$$-\frac{\omega_p^2}{2\,(\hat{\Omega}_\vartheta/\gamma)}\left(\frac{r_b}{a}\right)^2\left[\frac{X}{(1-R^2/a^2)\gamma^3}+\frac{a^2}{2r_o\gamma}\left[\beta^2+(1+\beta^2)\,\ell n\,\frac{a}{r_b}\right]\right] \tag{41}$$

Similarily, the last term in Eq. (32) must be replaced by

$$-\frac{\omega_p^2}{2\,(\hat{\Omega}_{zo}/\gamma)\,v_\vartheta}\left(\frac{r_b}{a}\right)^2\left[\frac{X_o}{(1-X_o^2/a^2)\gamma^3}+\frac{a^2}{2r_o\gamma}\left[\beta^2+(1+\beta^2)\,\ell n\,\frac{a}{r_b}\right]\right]. \tag{42}$$

Equations (41) and (42) have been derived under the assumption that $\dot{\gamma}/\gamma << \omega_w$. This assumption is valid because γ varies in the time scale of the slow beam motion. However, the γ in (41) and (42) is not the same with that at the injection point. The two γ s are related by

$$\gamma (X_o) - \gamma (X_{inj}) = - \frac{|e|}{mc^2} \int \vec{v} \cdot \vec{E} \, dt = \frac{|e|}{mc^2} [\Phi (X_o) - \Phi (X_{inj})], \tag{43}$$

where the potential Φ is computed from

$$\frac{|e|}{mc^2} \Phi (X) = \frac{\quad}{\quad} [\ln (1 + \frac{X}{r_o}) \ln (\frac{a}{r_b}) - \ln [1 - \frac{X^2}{a^2}]]. \tag{44}$$

In Eq. (43) the variation of γ associated with the toroidal electric field that is generated by the time changing self magnetic vector potential as the beam centroid moves in the transverse plane has been neglected.

III. Beam Trapping

The minimum requirements for trapping an electron beam in a toroidal device are:

1. During the first revolution around the major axis, i.e., in a time $\tau \leq (2\pi/\Omega_{zo/\gamma})$ the beam should drift along the guiding center orbit a distance greater than $r_b + r_{inj}$, where r_b is the minor radius of the beam and r_{inj} is the injector radius.

2. In a bounce period, τ_B i.e., in the time the beam completes a revolution around the equilibrium postion the guiding center orbit should be deformed radially near the injector at least as much as the distance $r_b + r_{inj}$.

3. Within a time interval of a few bounce periods the beam should drift near the minor axis of the torus, and

4. the radius of gyration around the guiding center should be substantially shorter than the radius of the guiding center.

The guiding center equations derived in the previous section provide a valuable guide in the development of a realistic trapping scheme for the following reasons. The beam drift velocity along the guiding center orbit can be optimized using Eqs. (30) and (31). From the shape of the guiding center orbit that can be determined from Eq. (38) and the bounce frequency, we can select the various parameters of the trapping field that will radially deform the guiding center orbit by the desirable amount so the beam wil not strike the injector after a bounce period. In addition, Eq. (32) gives the value of the betatron field required to drift the beam near the minor axis. Finally, the electron gyroradius around the guiding center can be minimized using Eqs. (28) and (29).

For the parameters of Table I, the value of the betatron field to have the equilibrium position of the beam on the minor axis of the torus can be computed from Eq. (32) and is approximately 48 G. Similarly, when the vertical field is 35G the equilibrium position X_o is located 10.2 cm from the minor axis of the torus (see Fig. 2d). Therefore, by increasing the betatron field as shown in Fig. 3, from 35 G to 48 G over a time period that is comparable to the beam bounce period, the beam equilibrium position will move from X_o = 10.2 cm to X_o = o. Fig. 4 shows the orbit of the reference electron for B_{zo} = 48 G, 35G and also for the combined field plotted in Fig. 3, This field consists of a 48G time in dependent field and a time dependent "trapping" field that varies as

$$B_{tr} = \begin{cases} B_{tro}\, e^{-(t-t_o)/\tau}, & \text{for } t > t_o \\ B_{tro}, & \text{for } t_o < t \end{cases},$$

where to is the trapping initiation time. The values of the various parameters of the "trapping" field for the results shown in Fig. 4 are listed in table II.

Over the first 20 nsec, i.e., over a revolution around the major axis the beam drifts 8 cm away from the injector, which is more than sufficient. However, the electron drifts around the new equilibrium position at $X_o = Z_o$ = o very slowly. The total time required to complete the bounce in Fig. 4 is in excess of 1.3 μsec.

To determine the sensitivity of the orbit to the initial azimuthal position of the injector, we made a series of runs with the injector always at the same X and Z but at different S positions. Figure 5 shows the results when the injector is moved from S = L/4 to S = o. As shown in table II the remaining

parameters for this run are identical to those of Fig. 4. It should be noticed that the final guiding center radius, i.e., when the electron gyrates around the $X_o = Z_o = o$ equilibrium position is appreciable smaller in Fig. 5 than in Fig. 4. The reason is that in Fig. 5 when the betatron field is 35G the constant of the motion K is zero, as manifested by the fact that the orbit passes through the minor axis. However, the constant K for the 35G orbit in Fig. 4 is positive. The trapping field increases the value of K by about the same amount in both runs. Thus, the final K is greater for the run of Fig. 4 than for the run of Fig. 5. Since the guiding center radius near the minor axis scales [see Eq. (39)] as the square root of K, it is reasonable to have a larger radius in Fig. 4 than in Fig. 5.

There is an additional difference between the results of these two runs, which is not apparent in the figures. In Fig. 5, at the injection point the torsatron field is directed downwards and thus the force $- e v_\theta B_z^t$ is radially outwards. As a result, the initial motion of the electron is outwards. In contrast, the $-ev_\theta B_z^t$ force at the injection point in Fig. 4 is radially inwards and so is the initial motion of the electron.

The results shown in Figures 4 and 5 were obtained for zero electron beam current. However, the trapping mechanism remains applicable even at high beam current I_b. Results are shown in Fig. 6 for I_b = 10 KA. The rest of the parameters for this run are listed in Table III. At high beam current the direction of the slow motion is opposite to that for $I_b = 0$, because the $\vec{E} \times \vec{B}$ drift exceeds the combined curvature and gradient drifts. Furthermore, in contrast to the low current case the equilibrium postion moves toward the major axis as the betatron magnetic field is reduced. This result is in agreement with Eq. (40).

Figure 7a shows the value of the vertical magnetic field required to confine the beam at its equilibrium position

(equilibrium magnetic field) when $I_b = 0$ and Fig. 7b shows the corresponding results for $I_b = 10$ KA and two different initial injection positions $X_{inj} = 0$ and 12.5 cm. The results of Fig. 7b have been obtained from Eq. (32) with the modification of Eq. (42). The various parameters for this run ($I_b = 10$ KA) are listed in Table IV. The equilibrium magnetic field depends upon the injection position because, as Eq. (43) indicates, γ at X_o is a function of X_{ing}. According to Fig. 7b, when $B_{zo} = 135$ G the equilibrium position X_o is at 112.5 cm. Similarily, when $B_{zo} = 119$ G the equilibrium position is at $X_o \approx 107$ cm and finally when $B_{zo} = 104$ G the equilibrium position is located near the minor axis.

In Figure 6, the betatron and trapping field have the same polarity and thus until the trapping is initiated, i.e., for the first 200 nsec the total vertical field is 119 G and therefore the equilibrium position is at 107 cm. For comparison the orbit of the reference electron for a time independent $B_{zo} = 119$ G is also shown in Fig. 6. By decreasing the total vertical field from 119 G to 104 G over a time period that is shorter than the beam bounce period, the beam equilibrium postion moves near the minor axis and the beam is trapped.

IV. Conclusions

For $\omega_w < (\Omega_{\theta/\gamma})$, we have derived two equations that describe the nonlinear, transverse motion of the guiding center of the reference electron that is located at the beam centroid. Using these equations we have obtained nonlinear expression that predicts very accurately the beam equilibrium postion, even when $2 \alpha R > 1$. Furthermore, by integrating analytically the guiding center equations, we have obtained a constant of the motion that predicts accurately the guiding center orbits in the transverse plane.

With the insight provided by these analytical results, we were able to develop a realistic trapping scheme that does not require the presence of a resistive wall and therefore is compatible with the relative slow acceleration of the modified betatron.

The proposed trapping scheme opens the possibility of adding strong focusing in a modified betatron accelerator. Such focusing may have several beneficial effects on the device, because it

- will alleviate the energy mismatch

- could alleviate the beam displacement associated with the diffusion of self magnetic field

- will improve the current carrying capabilities of the device without requiring injection at higher energies.

Table I
Parameters of the runs shown in Fig. 2.

Torus Major Radius r_0(cm)	=100
Winding Minor Radius ρ_0(cm)	= 18
Toroidal Chamber Minor Radius a(cm)	= 20
$\alpha = 2\pi/L$ (cm^{-1})	= 0.1
Field Strength Factor ε_t	= -0.04275
Winding Current I (kA)	= 25
ℓ	= 2
Torsatron Toroidal Field B_s^{ex}(kG)	= 1.0
Additional Toroidal Field B_s^{ex} (kG)	= 3.0
Betatron Field B_{zo} (G)	= 35
Ext. Field Index n	= 0.5
Beam Electron Density $n_0(cm^{-3})$	= 0
Initial γ	= 2.96

Table II

		Fig. 4	Fig. 5
Torus Major Radius r_o(cm)	=	100	100
Winding Minor Radius ρ_o(cm)	=	18	18
Toroidal Chamber Minor Radius a(cm)	=	20	20
$\alpha = 2\pi/L$ (cm^{-1})	=	0.1	0.1
Field Strength Factor ε_t	=	-0.04275	-0.04275
Winding Current I (kA)	=	25	25
ℓ	=	2	2
Torsatron Toroidal Field B_s(kG)	=	1.0	1.0
e-Fold time τ(nec)	=	100	100
Trapping Initiated at Time (nsec)	=	100	100
Trapping Field Amplitude B_{tr}(G)	=	-13	-13
Additional Toroidal Field B_s^{ex} (kG)	=	3.0	3.0
Betatron Field B_{zo}(G)	=	48	48
Ext. Field Index n	=	0.5	0.5
Electron Beam Current I_b (kA)	=	0	0
Initial γ	=	2.96	2.96
Initial Positions (cm) X(t=0)	=	14	14
Z(t=0)	=	0	0
S(t=0)	=	15.7	0
Initial Velocities $\dot{X}$(t=o)	=	0	0
$\dot{Z}$(t=o)	=	0	0
v_ϑ	=	0.941c	0.941c

Table III

Parmeters of the run shown in Fig. 6

Torus Major Radius r_o (cm)		=	100
Winding Minor Radius b_o (cm)		=	18
Toroidal Chamber Minor Radius a (cm)		=	16
$\alpha = 2\pi/L$ (cm^{-1})		=	0.1
Field Strength Factor ε_t		=	-0.04275
Winding Current I (kA)		=	25
ℓ		=	2
Torsatron Toroidal Field B_s (kG)		=	1.0
e-Fold time τ (nsec)		=	100
Trapping Initiated at Time (nsec)		=	200
Trapping Field Amplitude B_{tr} (G)		=	15
Additional Toroidal Field B_s^{ex} (kG)		=	3.0
Betatron Field B_{zo} (G)		=	104
Equilibrium Mag. Field at Inj. B_{eq} (G)		=	135
Ext. Field Index n		=	0.5
Electron Beam Current I_b (kA)		=	10
Initial γ		=	2.96
Minor Beam Radius r_b (cm)		=	1.0
b/γ		=	0.21
Initial Positions (cm)	$X(t = 0)$	=	13
	$Z(t = 0)$	=	0
	$S(t = 0)$	=	15.7
Initial Velocities	$\dot{X}(t = 0)$	=	0
	$\dot{Z}(t = 0)$	=	0
	v_ϑ	=	0.941c

Table IV

Parmeters of the run shown in Fig. 7

Torus Major Radius r_o (cm)		=	100
Winding Minor Radius ρ_o(cm)		=	18
Toroidal Chamber Minor Radius a (cm)		=	16
$\alpha = 2\pi/L$ (cm^{-1})		=	0.1
Field Strength Factor ε_t		=	-0.04275
Winding Current I (kA)		=	25
ℓ		=	2
Torsatron Toroidal Field B_s (kG)		=	1.0
Additional Toroidal Field B_s^{ex} (kG)		=	3.0
Ext. Field Index n		=	0.5
Electron Beam Current I_b (kA)		=	10
Initial γ		=	2.96
Minor Beam Radius r_b (cm)		=	1.0
ν/γ		=	0.21
Initial Positions (cm)	$X(t = 0)$	=	14
	$Z(t = 0)$	=	0
	$S(t = 0)$	=	0
Initial Velocities	$\dot{X}(t = 0)$	=	0
	$\dot{Z}(t = 0)$	=	0
	v_ϑ	=	0.941c

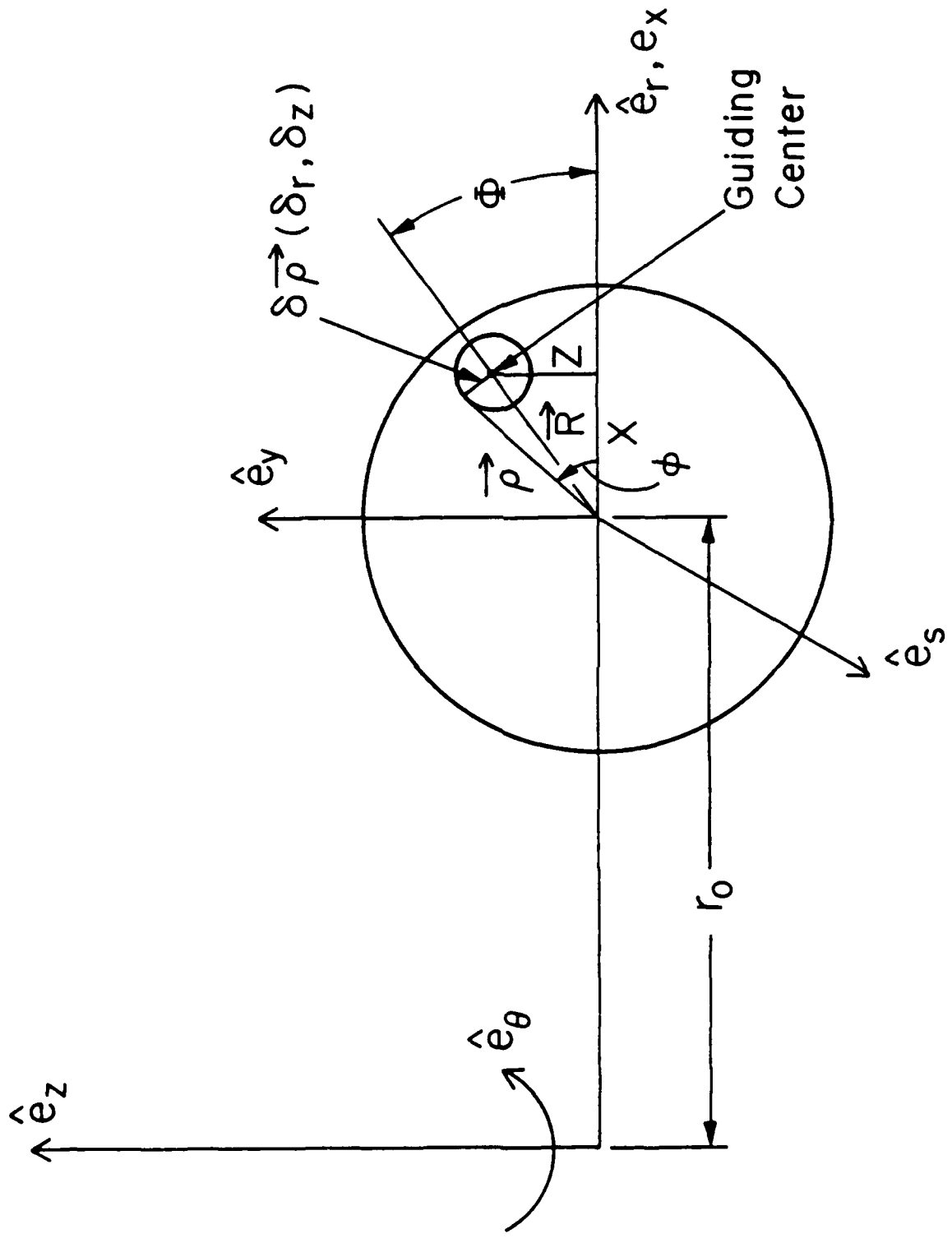

Fig. 1 — The various systems of coordinates used in the analysis

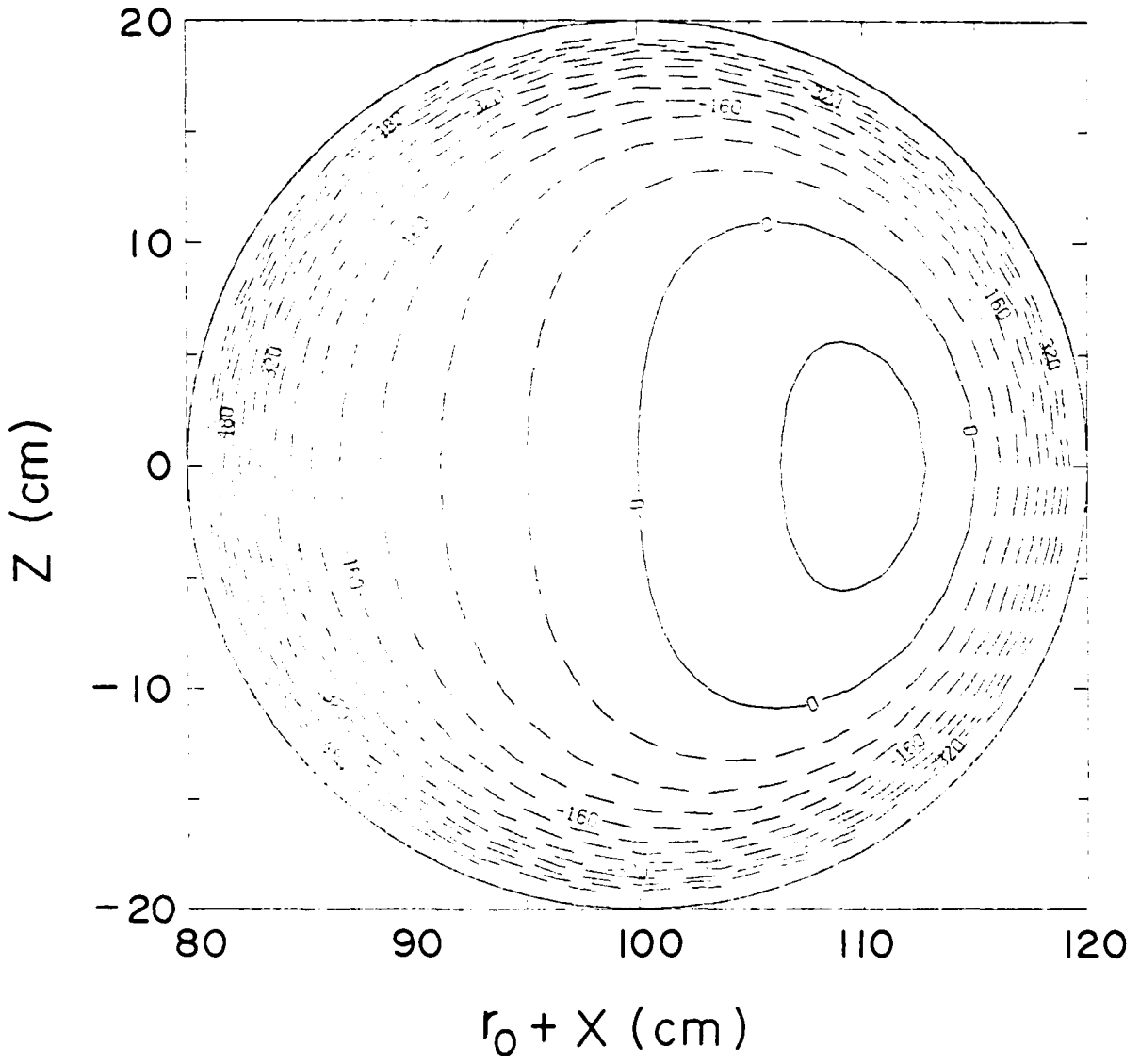

Fig. 2(a) — Guiding center orbits from Eq. (38) for several values of constant K for the parameters listed in Table I

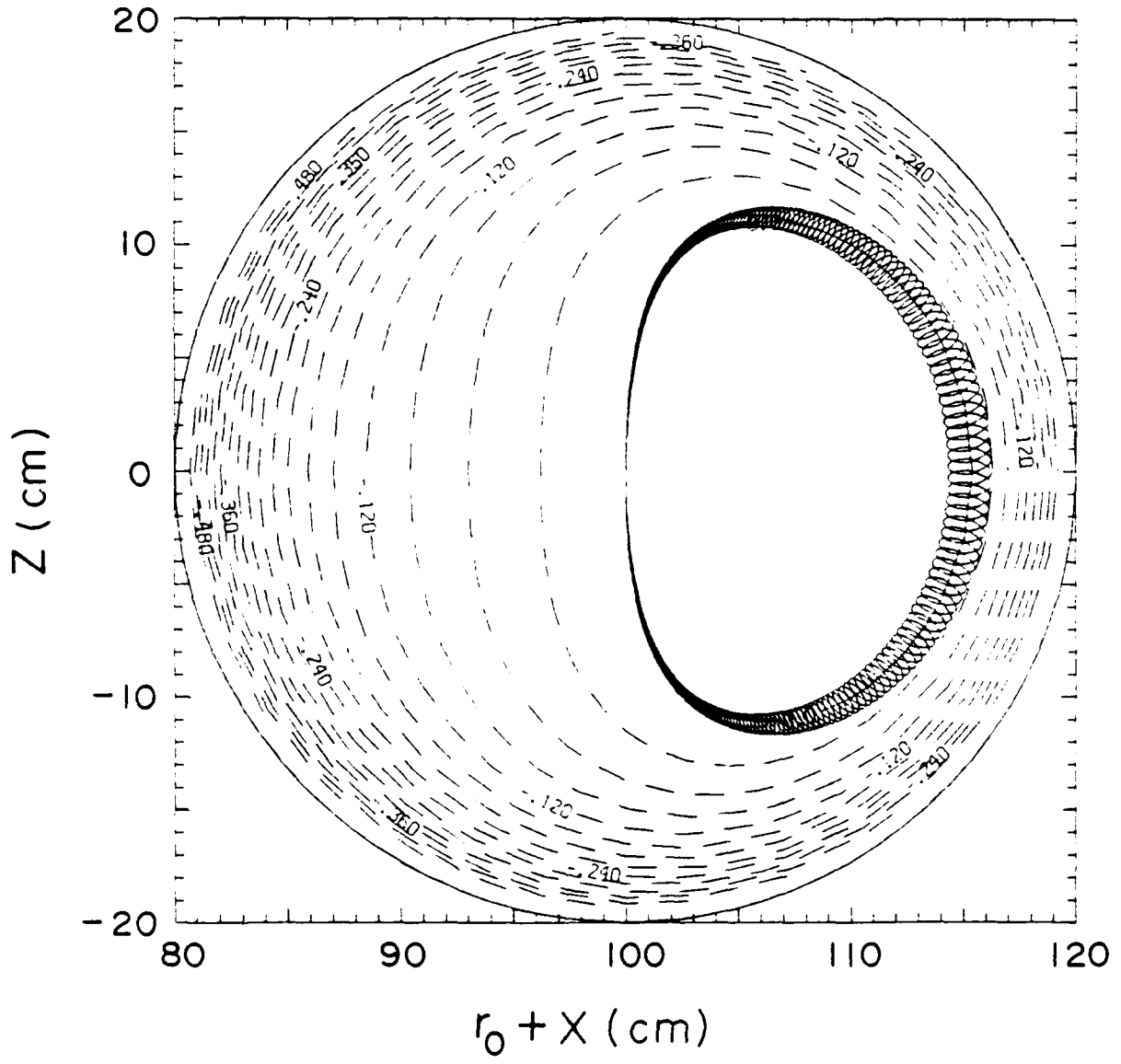

Fig. 2(b) — An electron beam orbit obtained from the numerical integration of orbit equations superimposed on the K = 0 guiding center orbit of Fig. 2(a). It is apparent that the constant of the motion predicts accurately the guiding center motion.

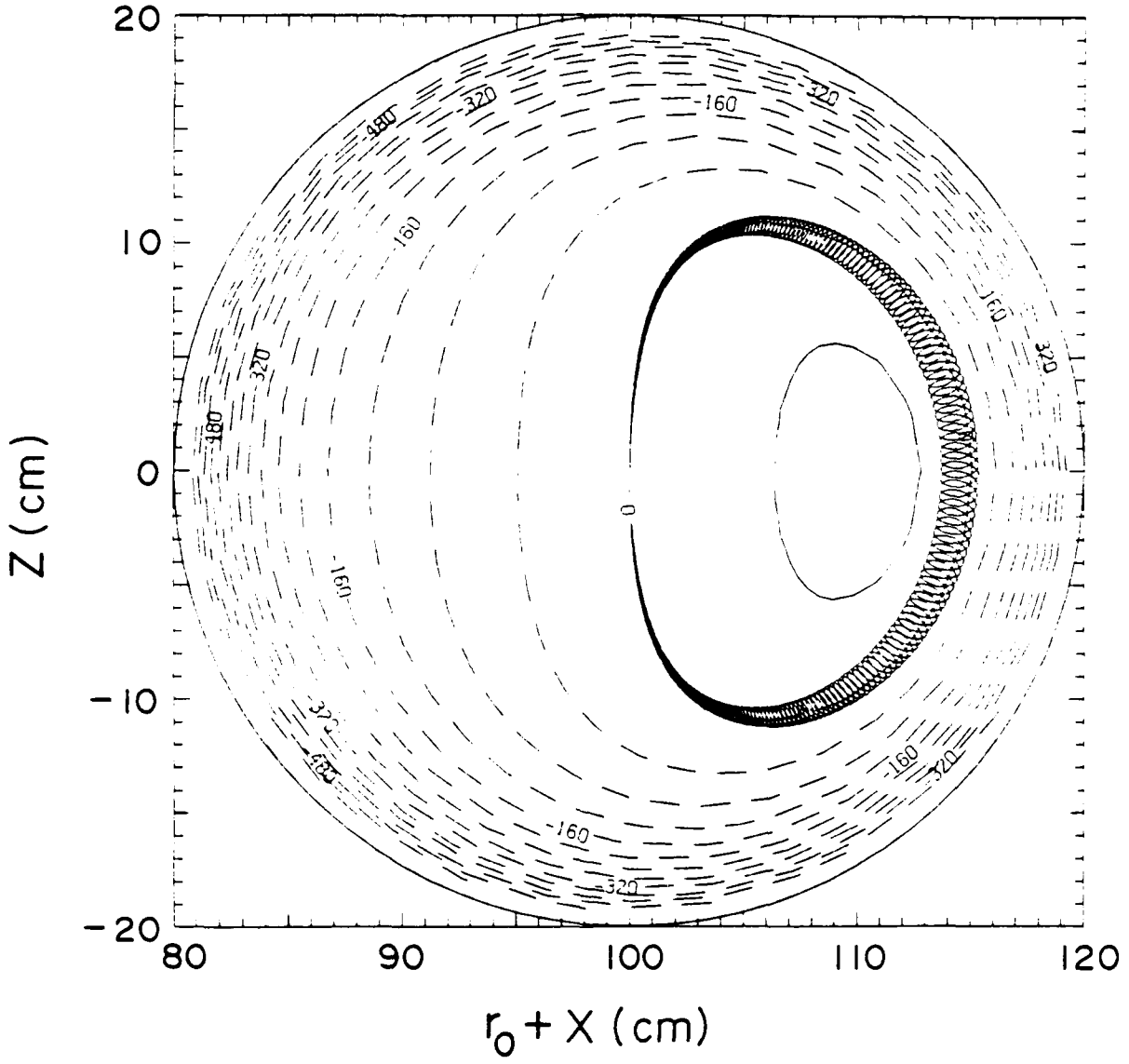

Fig. 2(c) — Same as in Fig. 2(b), but with the toroidal corrections of the torsatron field included in the numerical integration of orbit equations

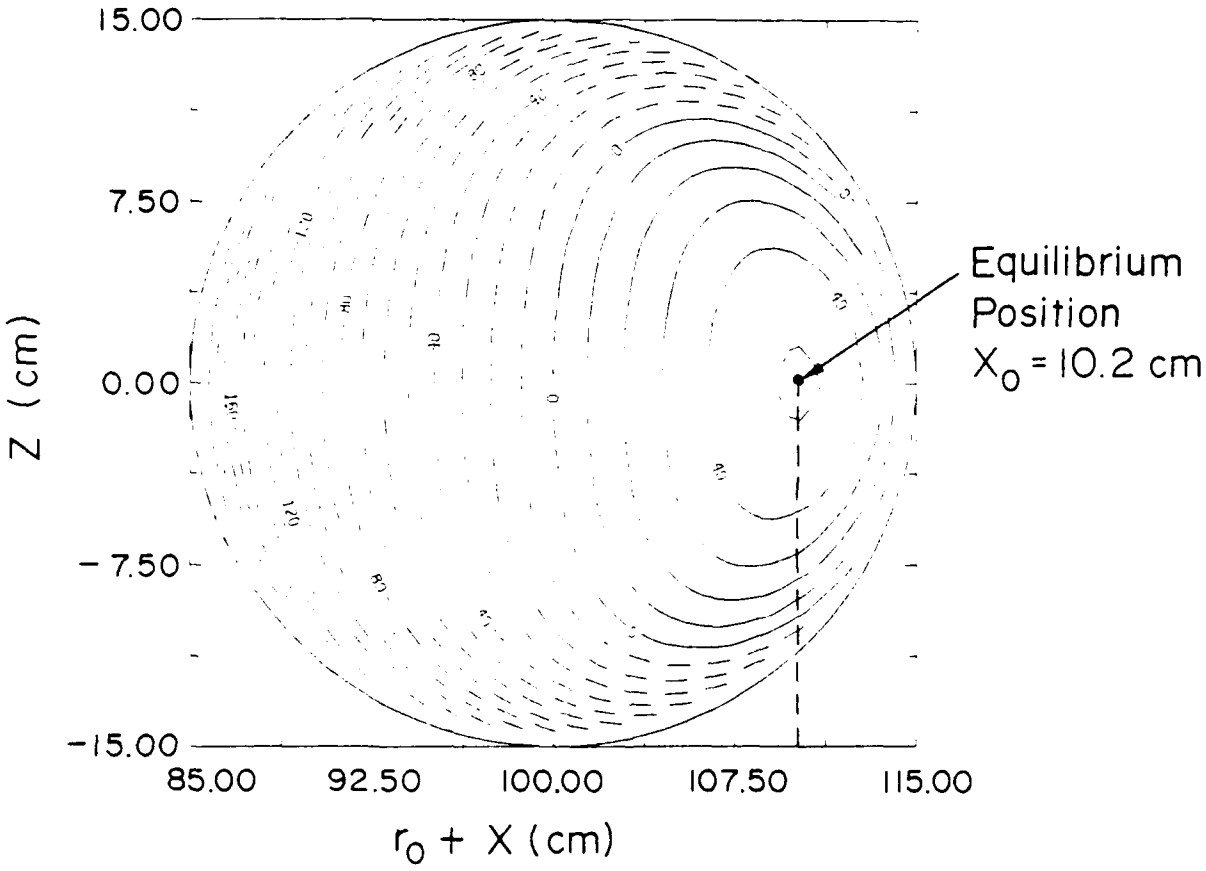

Fig. 2(d) — As Fig. 2(b), but a finer scale

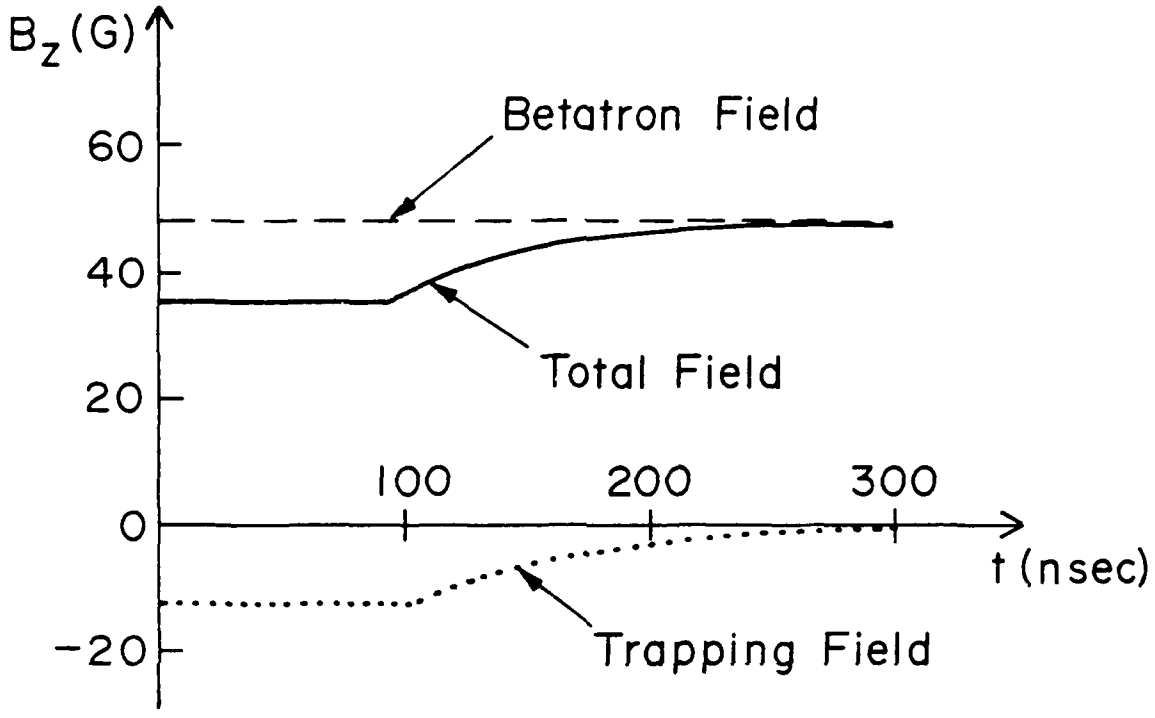

$$B_{tr} = \begin{cases} B_{tro}\, e^{-(t-t_0)/\tau}, & \text{for } t \geq t_0 \\ B_{tro}, & \text{for } t \leq t_0 \end{cases}$$

Fig. 3 — Betatron, trapping and total vertical field as a function of time

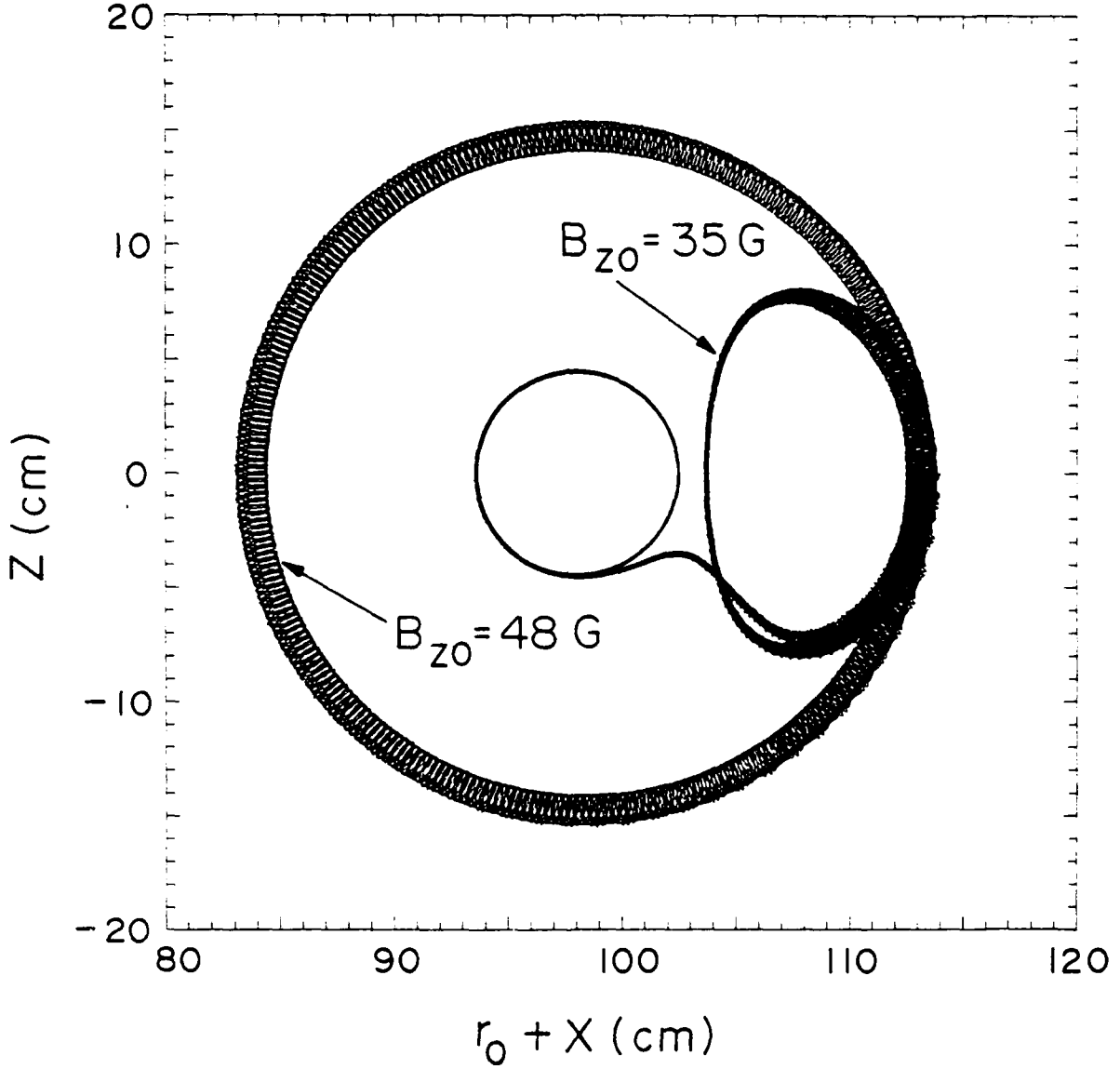

Fig. 4 — Orbit of reference electron at the beam centroid injected at 114 cm from the major axis when B_{zo} = 35 G = constant, B_{zo} = 48 G = constant and in the presence of the trapping magnetic field. The various parameters for this run are listed in Table II.

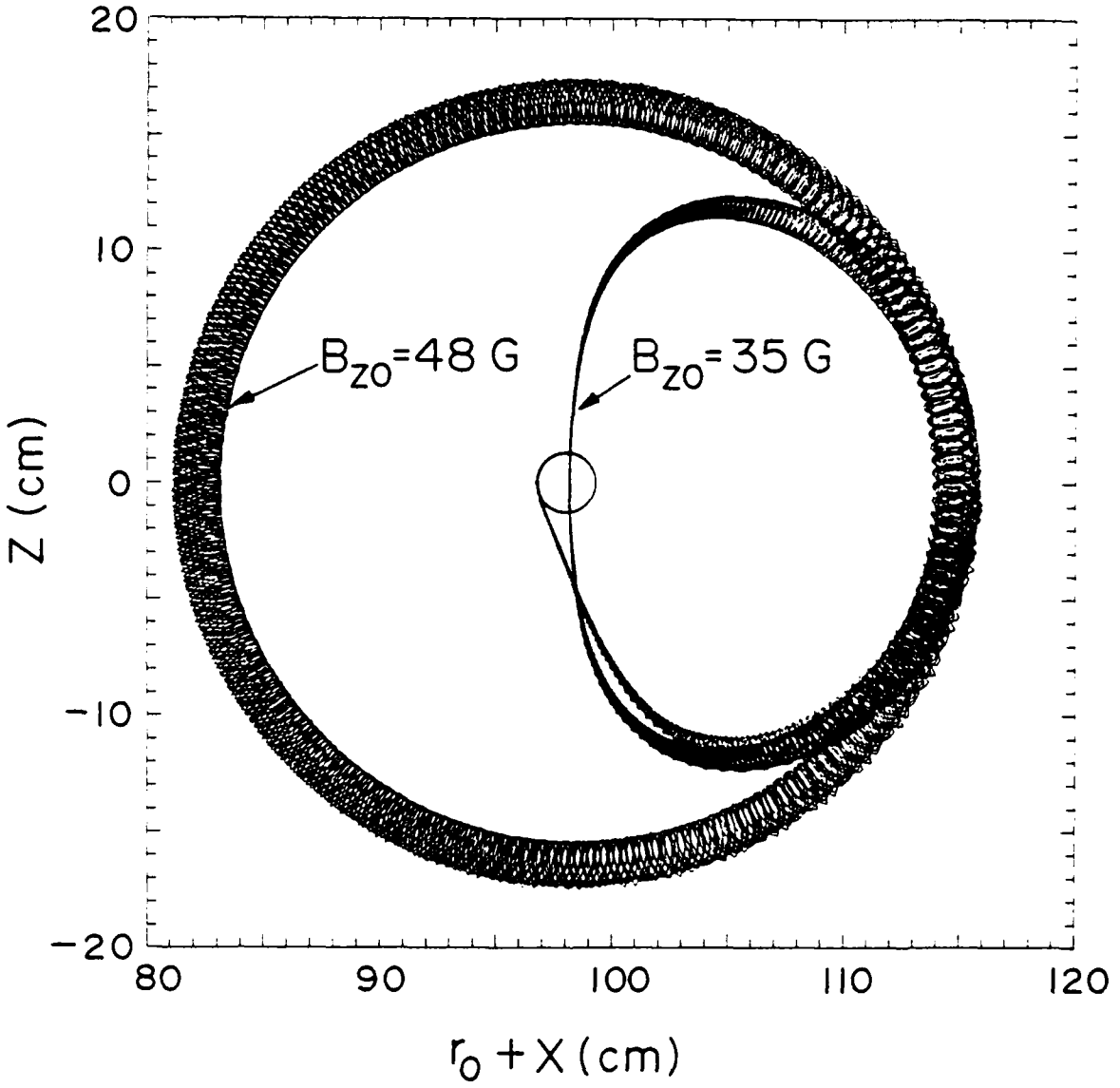

Fig. 5 — As in Fig. 4, but with the injector at a new initial toroidal position (S = 0). The various parameters for this run are listed in Table II.

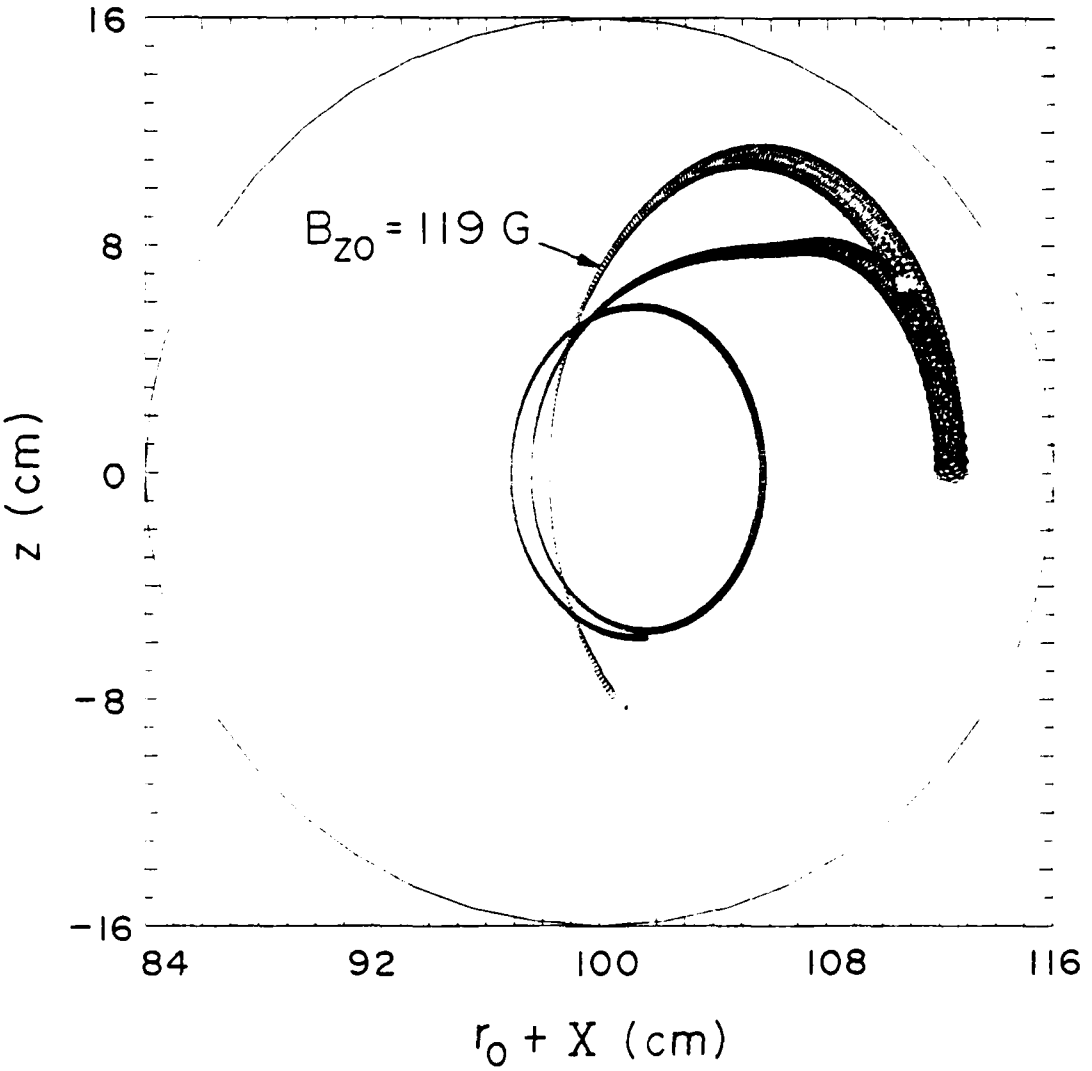

Fig. 6 — Orbit of reference electron located at the beam centroid injected at 113 cm from the major axis when B_{zo} = 119G (constant in time) and in the presence of the trapping magnetic field. The various parameters for this run are listed in Table III. Since the orbit of the fast motion of the particle has a 1 cm diameter, the average position of the particle (guiding center) and the injection position are different by about 0.5 cm.

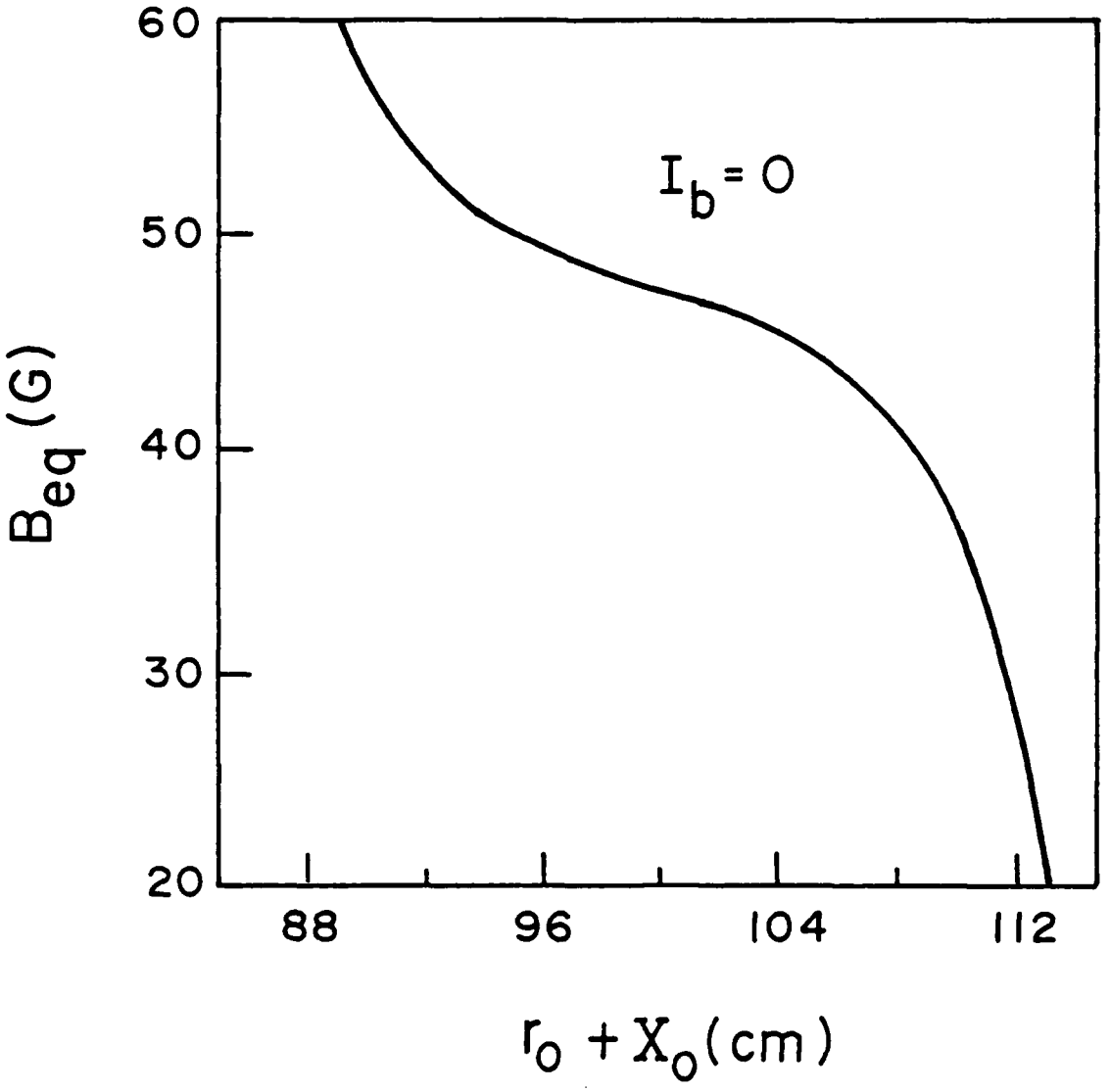

Fig. 7 — Vertical magnetic field required to confine the beam at its equilibrium position as a function of the equilibrium position for $I_b = 0$ (Fig. 7a) and $I_b = 10$ KA (Fig. 7b). The various parameters for these figures are listed in Table IV.

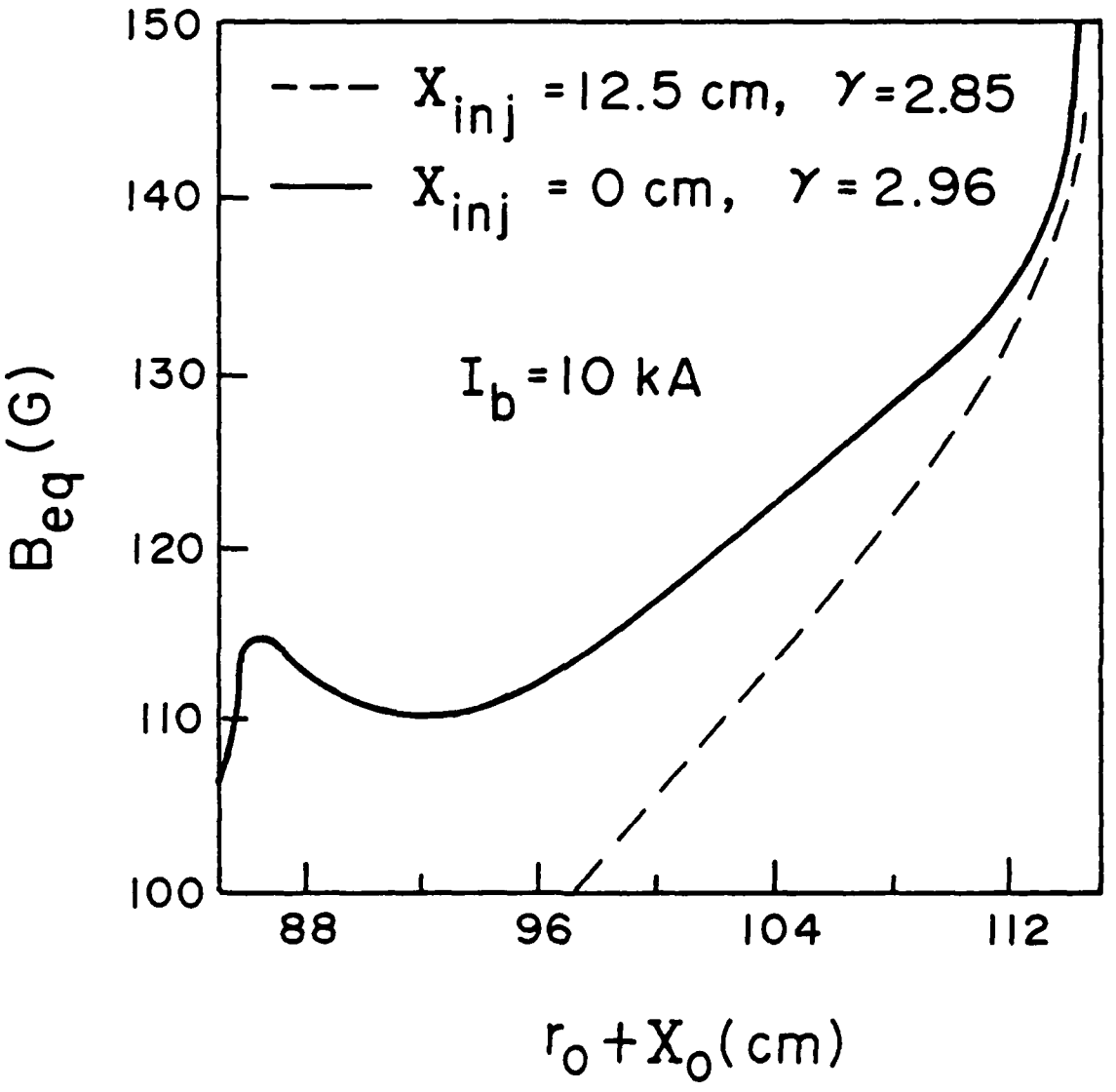

Fig. 7 (Cont'd) — Vertical magnetic field required to confine the beam at its equilibrium position as a function of the equilibrium position for $I_b = 0$ (Fig. 7a) and $I_b = 10$ KA (Fig. 7b). The various parameters for these figures are listed in Table IV.

References

+ Supported by SDIO and ONR

Δ Science Applications Int. Corp. McLean, Va. 22102

Sachs/Freeman Associates, Bowie, Md. 20715

1. P. Sprangle and C.A. Kapetanakos, J. Appl. Phys. 119, (1978)

2. C.A. Kapetanakos, P. Sprangle, D.P. Chernin, S.J. Marsh and I Haber, Phys. Fluids, 26, 1634 (1983)

3. D. Chernin and P. Sprangle, Part. Accel. 12, 85 (1982)

4. W. Manheimer and J. Finn, Part. Accel. 14, 29 (1983)

5. C. Agritellis, S.J. Marsh and C.A. Kapetanakos, Part. Accel. 16, 155 (1985)

6. C.A. Kapetanakos, S.J. Marsh, Phys. Fluids, April (1985)

7. J. M. Grossman, T.M. Finn and W. Manheimer Phys. Fluids 29, 695 (1985)

8. T.M. Grossmann and W.M. Manheimer Part. Accel. 16, 185 (1985

9. W.M. Manheimer, Part. Accel. 13, 209 (1983)

10. D. Chernin and P. Sprangle, Part. Accel. 12, 101 (1982)

11. P. Sprangle and C.A. Kapetanakos, Part. Accel 14, 15 (1983)

12. P. Sprangle and D. Chernin, Part. Accel. 35, 15 (1984)

13. C.A. Kapetanakos, P. Sprangle and S.J. Marsh, Phys. Rev. Letts. 49, 741 (1982)

14. F. Mako, W. Manheimer, D. Chernin, F.Sandal and C.A. Kapetanakos, Phys. Fluids

15. B. Hui and T.T. Lau, Phys. Rev. Letts. 53, 2024 (1984)

16. N. Rostoker, Comments on Plasma Physics, Vol. 6, P. 91 (1980)

17. G. Barok and N. Rostoker, Phys. Fluids 26, 856 (1983)

18. R.C. Davidson and H.S. Uhm, Phys. Fluids 25, 2089 (1982)

19. H.S. Uhm and R.C. Davidson, Phys. Fluids 25, 2334 (1982)

20. H.S. Uhm, R.C. Davidson and J. Petilo, Phys. Fluids (1985)

21. H. Ishizuka, G. Lindley, B. Mandel Baum, A. Fisher and N. Rostoker, Phys. Rev. Letts. 53, 266 (1984)

22. J. Golden, J. Pasour, D.E. Pershing, K. Smith, F. Mako, S. Slinker, F. Mora, N. Orick, R. Altes, A. Fliflet, P. Champney and C.A. Kapetanakos, Proceedings of IEEE Trans. Nucl. Scie.) NS-30, 2114 (1983)

23. C.W. Roberson, A. Mondelli and D. Chernin, Phys. Rev. Letts. 50, 507 (1983)

24. C.A. Kapetanakos, P. Sprangle, S.J. Marsh, D. Dialetis, C. Agritellis and A Prakash, Part. Accel., 1985

25. P. Sprangle and C.A. Kapetanakos, Part. Accel., 1985

END

FILMED

1-86

DTIC